IOP Publishing Journal of Radiological Protection

J. Radiol. Prot. **30** (2010) 491–512 doi:10.1088/0952-4746/30/3/005

Modelling particle retention in the alveolar–interstitial region of the human lungs

D Gregoratto, M R Bailey and J W Marsh

Centre for Radiation, Chemical and Environmental Hazards, Health Protection Agency, Chilton, Didcot, Oxon OX11 0RQ, UK

E-mail: demetrio.gregoratto@hpa.org.uk

Received 22 January 2010, in final form 21 April 2010, accepted for publication 14 May 2010
Published 8 September 2010
Online at stacks.iop.org/JRP/30/491

Abstract

Better information is available now on long-term particle retention in the human lungs than there was in 1994, when the human respiratory tract model (HRTM) was adopted by the International Commission on Radiological Protection (ICRP). Three recent studies are especially useful because they provide such information for groups of people who inhaled very similar aerosols. For all three the HRTM significantly underestimates lung retention of insoluble material. The purpose of this work was to improve the modelling of long-term retention in the deep lung. A simple physiologically based model developed to predict lung and lymph node particle retention in coal miners was found to represent lung retention in these studies adequately. Instead of the three alveolar–interstitial (AI) compartments in the HRTM, it has an alveolar compartment which clears to the bronchial tree and to a second compartment, representing the interstitium, which clears only to lymph nodes. The main difference from the HRTM AI model is that a significant fraction of the AI deposit is sequestered in the interstitium. To obtain default parameter values for general use, the model was fitted to data from the three recent studies, and also the experimental data used in development of the HRTM to define particle transport from the AI region for the first year after intake. The result of the analysis is that about 40% of the AI deposit of insoluble particles is sequestered in the interstitium and the remaining fraction is cleared to the ciliated airways with a half-time of about 300 days. For some long-lived radionuclides in relatively insoluble form (type S), this increased retention increases the lung dose per unit intake by 50–100% compared to the HRTM value.

(Some figures in this article are in colour only in the electronic version)

0952-4746/10/030491+22$30.00

1. Introduction

The human respiratory tract model (HRTM) (ICRP 1994a) has been applied to calculate inhalation dose coefficients and bioassay functions for workers and members of the public (ICRP 1994b, 1995, 1996, 1997). The model represents clearance of materials deposited in the respiratory tract as a combination of particle transport to the gastro-intestinal (GI) tract and lymph nodes, and absorption of dissolved material into the blood (except from the anterior nasal, ET_1, passage which is cleared by nose blowing). The HRTM provides particle transport clearance rates from each compartment, which apply to all materials. The model shown in figure 1 would describe the retention and clearance of a completely insoluble material. In general there is simultaneous dissolution and absorption to blood, which depends on the chemical form of the material, but in the HRTM it is assumed to occur at the same rate in all the compartments except ET_1.

Data from three recent studies are considered to provide better information on long-term particle clearance from the human lung than any available when the HRTM was developed, because they provide such information on groups of people who inhaled very similar aerosols: (i) an experiment in which retention was followed for 900 days (Philipson *et al* 1996); (ii) the 15 year follow up of a group of workers who inhaled particles containing ^{60}Co (Davis *et al* 2007); and (iii) the 35 year follow up of a group of workers who inhaled plutonium dioxide (ORAUT 2007). All show much slower clearance than the HRTM predicts. Their results, together with those on which the HRTM was based, were used here to develop a new compartment model of particle transport from the AI region.

The ICRP is producing documents on occupational intakes of radionuclides (OIR) which will provide new dose coefficients and bioassay functions, and therefore an opportunity for updating the HRTM (Bailey *et al* 2007). Other recent studies also enable more reliable parameter values to be chosen for particle transport from the extrathoracic airways (ET); bronchial (BB) and bronchiolar (bb) regions. The AI region is addressed in this paper. However, brief consideration is also given to the BB and bb regions in the following sections, because assumptions made about the extent of a slow phase of clearance in them affect the analysis of alveolar retention.

1.1. Alveolar–interstitial region

In the HRTM the AI region is represented by three compartments: AI_1, AI_2 and AI_3, which mainly clear to the GI tract via the bronchial tree (figure 1). When the model was developed, human lung clearance had been quantified in experimental studies up to about a year after inhalation (ICRP 1994a). Over this time, retention of the initial alveolar deposit (IAD) of insoluble particles typically follows a two-component exponential function: about 30% with a half-time of about 30 d, and the rest with a half-time of several hundred days, giving about 50% retention at 300 d. This information was used to define the parameter values for AI_1. Measurements of activity in the chest after occupational exposure, and of material in the lungs at autopsy, indicated that particles can be retained in the lungs for decades. However, the results were not used to set parameter values for AI_2 and AI_3 quantitatively, because it was possible that the published *in vivo* studies represented unusually slow lung clearance (ICRP 1994a, paragraph E193). Instead, it was noted (ICRP 1994a, paragraph E217) that: 'The fraction of the AI deposit that goes to AI_3 (a_3) is not easily quantified. Since only 50% IAD is retained at 300 d, a_3 is less than 0.5. Since there is measurable thoracic retention at 5000 d after intake in some subjects (figure E.10), a_3 is likely to be at least a few per cent of the IAD. As a rounded value it is assumed that $a_3 = 0.1$, and, hence, by difference, that $a_2 = 0.6$'.

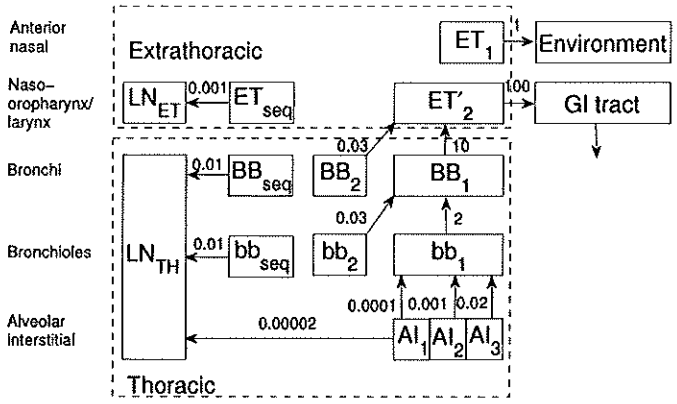

Figure 1. HRTM compartmental model for particle transport from the human respiratory tract. Rates (d^{-1}) shown alongside arrows are reference values (ICRP 1994a).

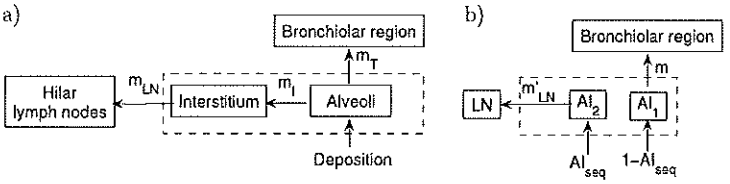

Figure 2. (a) Kuempel *et al* (2001) model for the gas-exchange region of the human respiratory tract. (b) 'Equivalent' model (AI_1 and AI_2: alveolar–interstitial region, LN: lymph nodes).

Kuempel *et al* (2001) developed a simple model of long-term lung and lymph node particle retention (figure 2(a)) with separate alveolar and interstitial compartments, that clear to the bronchiolar region and hilar (thoracic) lymph nodes respectively, reflecting the physiological processes. It was applied to a group of US coal miners for whom there were exposure histories on which to assess dust deposition rates, and autopsy measurements of lung dust concentration (and in about 50% of cases lymph node concentration). The model was considered to be the simplest consistent with the data, and no evidence was found for impaired clearance at high lung loadings.

Values for the transport rates were estimated. Deposition in the alveolar region was calculated for inhalation of particles with mass median aerodynamic diameter of 5 μm, by a reference worker (ICRP 1994a). Data from experimental human studies in the literature, as used to define compartment AI_1 in the HRTM, were used to optimise the rate m_T to the bronchiolar region. The transfer rate from the interstitium to the lymph nodes was chosen in order to give the correct ratio for the contents of lung and lymph nodes at the end of life. For the miners studied, Kuempel *et al* (2001) obtained optimised parameter values by which the alveolar compartment clears to the bronchiolar region ($m_T = 0.001\ d^{-1}$), and to the interstitium ($m_I = 4.7 \times 10^{-4}\ d^{-1}$) from which particles clear to the lymph nodes ($m_{LN} = 10^{-5}\ d^{-1}$). These are described as 'default' values in the rest of this paper. The average value for the ratio of the concentration of dust in lymph nodes $[LN]$ to the concentration in lungs $[L]$ evaluated with these parameter values is $[LN]/[L] \approx 7$ at 10 000 days after inhalation.

A key feature of Kuempel *et al* (2001) model is that a large fraction of IAD becomes sequestered in the interstitium, approximately $m_I/(m_T + m_I)$. For the US coal miners about

70% IAD is cleared from the lungs in about 4000 days, but the remaining 30% stays almost indefinitely in the interstitium and is only slowly cleared to the lymph nodes. Kuempel *et al* noted that the HRTM underestimated lung retention in the miners by about a factor of four (Kuempel and Tran 2002). The model has been independently validated on data for UK miners (Tran and Buchanan 2000).

We tested this AI model (for simplicity referred to as the 'Kuempel' model in the rest of the paper) on the measurement data described in section 2.1, optimising the transport rates m_T and m_I to obtain the best fit to the *in vivo* (whole body or lung) and *in vitro* (urine and faeces) measurements. The set of linear equations shown in Kuempel *et al* (2001) for the number, or mass, of dust particles in the model compartments, A (alveolar region), I (interstitial region) and LN (lymph nodes), are also valid for the activity of the inhaled particles. For an insoluble material and for unit IAD, the total activity in the alveolar, interstitium and lymph nodes compartments is:

$$[A + I + LN](t) = e^{-mt} + \frac{m_I}{m}(1 - e^{-mt})$$
$$= \frac{m_I}{m} + \frac{m_T}{m}e^{-mt} = AI_{seq} + (1 - AI_{seq})\, e^{-mt}$$

where $m = m_T + m_I$ and $AI_{seq} = m_I/(m_T + m_I)$. The first expression in the equation shows the contribution from the compartments A and $(I + LN)$ respectively, while the second expression emphasises the fact that the total activity is the sum of the fraction AI_{seq} which is finally sequestered in the interstitium and lymph nodes plus the complementary fraction $1 - AI_{seq}$ which clears with an overall rate m. The parameters AI_{seq} and m, in fact, may be used to define an equivalent model, represented in figure 2(b), to describe the overall retention in the alveolar–interstitial region plus lymph nodes. There are, of course, differences between the two formulations in the distribution of the material among the three compartments at any time, but not in the total amount (see also section 4). In the Kuempel model the default values of these parameters are $AI_{seq} = 0.32$, $m = 0.0015\ d^{-1}$. In the following, we will often refer to the parameters AI_{seq} and m, instead of m_T and m_I, because of their more intuitive role in the interpretation of lung measurements. Their values were determined by fitting to the *in vivo* data, while the transfer rate from interstitium to lymph nodes was determined independently.

1.2. Bronchial and bronchiolar regions

The HRTM includes a slow phase of clearance of particles deposited in the BB and bb regions (figure 1): compartments BB_2 and bb_2 clear at a rate of $0.03\ d^{-1}$, corresponding to a half-time of 23 days. This is relevant here in assessing the IAD and clearance from the AI region during the first few months after intake. In developing the HRTM, it was assumed that lung retention at seven days after intake provides a good estimate of IAD. However, in some situations the HRTM predicts significant retention in the BB and bb regions at seven days, and hence clearance from these regions over the following weeks.

The results of recent volunteer studies suggest slow clearance occurs mainly in the bronchioles (Bailey *et al* 2007). In particular, according to the experiments and analysis of Falk *et al* (1999), lung clearance over the first six months can be described by: (i) a rapid phase over the first day, associated with mucociliary clearance from BB and bb, (ii) an intermediate phase with a half-time of about four days associated with a fraction of the deposit in the bb region (25% for the conditions of the experiments) and (iii) a much slower phase associated with the AI region. For the analyses in section 3 below it is assumed that the BB region has only the fast clearance phase (half-time 2 h, as for BB_1 in the HRTM), and that the bb region has both a fast phase (half-time 8 h, as for bb_1 in the HRTM) and a slow phase of four days

(instead of 23 days as for bb_2 in the HRTM) with 25% of the deposit in the bb region subject to slow clearance. For simplicity this is described as the 'Falk' model in the rest of this paper.

1.3. Transfer to lymph nodes

In the HRTM (figure 1), the rate of transfer to the thoracic lymph nodes (LN_{TH}) from the AI region was set at 0.000 02 d^{-1} in order to give a concentration ratio $[LN]/[L] \approx 20$ at 10 000 days after intake, as observed in autopsy studies of non-smokers (Kathren *et al* 1993). Allowance was first made for transfer from the BB and bb regions. A small fraction of the material deposited there (0.7%) was assumed to be sequestered in the airway wall, and from there transported to LN_{TH} at a rate of 0.01 d^{-1}. These parameter values were based on studies in rats, the only species for which it was known to be quantified. New values for these parameters were proposed by Bailey *et al* (1997) based on experiments by Takahashi *et al* (1993) in dogs and monkeys: the fractions going to BB_{seq} and bb_{seq} are reduced to 0.05% and the clearance rates from BB_{seq} and bb_{seq} to LN_{TH} reduced to 0.001 d^{-1}. These changes were applied in the analyses here (section 3) but do not significantly affect the results. However, they reduce the amount of material cleared to LN_{TH} from BB and bb. Changes to the values of these parameters were included in calculating the rate from the AI region to the LN_{TH} to give the correct concentration ratio $[LN]/[L]$ for the proposed new AI model.

2. Materials and methods

2.1. Datasets

Philipson *et al* (1996) followed lung retention in 10 volunteers for about 900 days after inhalation of ^{195}Au-labelled Teflon particles. The monodisperse aerosol (mean geometric diameter = 3.6 μm, AMAD = 5.3 μm and geometric standard deviation = 1.07) was inhaled at a flow rate of 1.8 $m^3\ h^{-1}$ (breathing or ventilation rate of 0.9 $m^3\ h^{-1}$). The material was extremely insoluble: the leakage of ^{195}Au from particles in water was less than 0.2% in one year, which corresponds to a dissolution rate of $s < 6 \times 10^{-6}\ d^{-1}$. Therefore, absorption to blood should not play an important role in lung clearance. Lung retention was followed for 900 days with two different detector systems (NaI and Ge). Activity measurements in faeces are also available at times over this period. The lung measurements started seven days after inhalation and are reported for each subject, as single exponential functions over each of two periods: 7–250 days and 250–900 days. These values represent the lung retention after correction for radioactive decay. There was a significant difference between the lung retention estimated from measurements obtained with the NaI and Ge detectors for the period 250–900 days, but measurements obtained with the system of NaI detectors were in good agreement with the faecal measurements and were chosen here for the analysis of lung retention. The lower activities measured with the Ge detector systems were attributed to its higher sensitivity to the location of the activity source and to translocation of material from lungs to lymph nodes during the measurement period.

A contamination incident in which seven workers had a simultaneous inhalation of very insoluble particles containing ^{60}Co (half-life 1924 days), provided a dataset which is reasonable to assume to be representative for nuclear industry workers. Whole body measurements were carried out over a period of 15 years and early urine and faecal data are available for each individual. An analysis of the results was published by Davis *et al* (2007). Data for each case can also be found in the IDEAS Internal Contamination database (Hurtgen *et al* 2007) as cases 227–233.

Cases of accidental intake of plutonium oxides at the Rocky Flats Plant (RFP) show long-term lung retention of plutonium which exceeds that predicted by the ICRP respiratory tract model for insoluble (type S) material. Nine cases were analysed here, which were considered in a previous study based on lung measurements and reported in a National Institute for Occupational Safety and Health (NIOSH) Technical Document (ORAUT 2007). In addition to the lung measurements, data for plutonium activity in urine were provided by NIOSH and are included in the present analyses. For all cases, lung measurements were based on the 60 keV photon peak of ^{241}Am. Given the isotopic composition of the plutonium, based on the general mixture of plutonium handled at RFP, the count rate data were then converted to plutonium activity. The errors on the measurements were reported to be normally distributed with a standard deviation of about 30% of the measured value for most of the cases. This value is similar to the value recommended by the IDEAS Guidelines for *in vivo* measurements with photon energies in the range 20 keV $< E <$ 100 keV. Decorporation therapy with DTPA (diethylene triamine pentaacetic acid) was initially applied to the first contaminated cases but was discontinued and not used on the other cases because it did not enhance plutonium excretion in the urine, probably because of the low solubility of the material.

Six of the RFP cases were exposed to plutonium from a fire in October 1965 (Mann and Kirchner 1967). The plutonium consisted of 'high-fired' PuO_2. Particle size measurements of air samples indicated a mass median diameter of 0.32 μm with a geometric standard deviation of 1.83. The corresponding AMAD is about 1 μm, given a particle density of $\rho_m = 11.5$ g cm^{-3}, ($d_{ae} = d\sqrt{\rho_m/\chi}$, using a shape factor $\chi = 1.5$). The amount of ^{241}Am in the mixture was measured late in the day of the fire and is 1830 parts-per-million (ppm) by mass. The ratio of the activity of ^{241}Pu to the alpha activity of the other plutonium isotopes is 5.1. For the other three cases there was no specific information on the particle size and the default AMAD of 5 μm was assumed. Measurements are available for up to 30 years.

2.2. *Methods*

2.2.1. Calculation of deposition. For the Teflon and PuO_2 studies, reported information on the aerosol size distribution was used with the HRTM deposition model to calculate fractional deposition of inhaled material in each region. For the cobalt-60 study, no direct measurement of the aerosol particle size was available. However, measurements of early faecal excretion and whole body retention enabled the 'effective AMAD' (ICRP 2002, Marsh *et al* 2008) to be calculated. The ratio of faecal excretion in the first few days to the initial lung activity reflects deposition in the upper and lower respiratory tracts, and over a wide size range increases with increasing AMAD. The 'effective AMAD' is the value of AMAD which gives the ratio observed, for a given breathing rate (BR, here taken to be 1.2 m^3 h^{-1}). For this study it was calculated from the early cumulative faecal data ($t < 72$ h) and the whole body measurement at $t = 10$ days. For an insoluble material, these quantities are good approximations to the amounts deposited in the upper and lower respiratory tract respectively. The lung deposition was calculated with LUDEP (Jarvis and Birchall 1994).

2.2.2. Calculation of retention. Available experimental data consist of time-series measurements of activity in lung or whole body, and also of activity excreted in urine and/or faeces for each subject. Therefore, to compare the model prediction with all the available data, both the lung model and the biokinetic model for systemic tissues must be solved to estimate the initial intake. The systemic models for cobalt (^{60}Co) and plutonium (^{239}Pu) are

provided by ICRP publications (ICRP 1993) and Leggett *et al* (2005) respectively, while the HRTM was modified as follows: the Falk model (section 1.2) was adopted for the bronchial (BB) and bronchiolar (bb) regions and the Kuempel model structure (section 1.1) for the AI region. Before solving the model, assumptions or estimates of physical–chemical properties of the inhaled material (particle size, solubility) had to be made where no direct information was provided. These are discussed in section 3 for each cohort. The measurement errors, unless provided, were estimated following the IDEAS guidelines (Doerfel *et al* 2006). With a chosen model, i.e., with fixed values for its parameters, the unknown intake was estimated with the maximum-likelihood (ML) method, assuming normal or lognormal distributions for the measurement errors. This method was chosen because of the presence of data below the lower limit of detection (<LLD) (see appendix A); it is numerically equivalent to using the least squares (LS) method when there are no <LLD measurements, as was the case except for a small per cent of data within the ^{60}Co cohort. The lung + biokinetic model was solved as an eigenvalue problem (Polig 2001, Fell *et al* 2007) using the software GNU-Octave (Eaton 2002) and IMBA (Birchall *et al* 2007) was used as benchmark for the *in vivo* and bioassay predictions.

2.2.3. Maximum-likelihood parameter estimation. To obtain the best fit to the data, the model parameters were optimised by using the Levenberg–Marquardt (LM) method (Press *et al* 2007). This algorithm is often chosen as a reliable and powerful method to find the minimum (or maximum) of non-linear functions. Here the maximum of the log-likelihood was needed as a function of the model parameters conditional on the observed data $\log[L(\boldsymbol{p}|\boldsymbol{x})]$. This optimisation procedure was applied to each of the subjects of a given cohort. The LM method also incorporates the possibility to estimate the covariance matrix Σ_p of the parameters, which is regularly used in multiple linear regression to evaluate the parameter confidence regions (Draper and Smith 1998). In the more general case of non-linear regression, the parameter covariance matrix estimated by linearising the model around $\boldsymbol{p}_{\max}$ provides an approximation for the parameters' variance, correlation coefficients and confidence regions. Further details on the optimisation procedure are given in appendix B.

2.2.4. Posterior distribution estimation. The parameter uncertainties for the whole cohort were also analysed within a Bayesian framework. This required determination for each subject of the posterior distribution function, defined as the product of the likelihood function $L(\boldsymbol{p}|\boldsymbol{x})$ and the parameter prior distribution function $\pi(\boldsymbol{p})$. By adding the posterior distributions of each subject, i.e. by giving all the subjects the same weight, we obtained the posterior distribution for the whole cohort, which is a joint N-dimensional probability density function (PDF) for the N parameters. Two ways were followed to determine the likelihood function for each subject: a simple analytical approximation (multivariate normal distribution) and the exact mapping in the parameter space. The ML-LM (maximum likelihood-Levenberg Marquardt) procedure is computationally very efficient and does not require excessive computer memory or time but the accuracy of the approximated parameter likelihood function (and posterior distribution) generally depends on the number of data available and on how adequately the model describes the system. To obtain a more accurate solution, compared to the multinormal approximation, it is necessary to map the likelihood function in the parameter space. This could become computationally very expensive and usually one resorts to Monte Carlo methods (Miller *et al* 2002, Puncher and Birchall 2008) to calculate the main statistics (mean and moments of higher order). Given that we optimised not more than four parameters simultaneously, and that in most cases the ML-LM solution fitted the data very well, we have mapped the likelihood function selecting the points on a Cartesian grid in a guided way. Further details on the determination of the posterior distribution are given in appendix B.

Table 1. Lung retention (%) with respect to the retention at day seven. Experimental data (Exp) and retention predicted by the HRTM for the material and inhalation parameters used in the Philipson *et al* (1996) study are shown: lung retention for the default HRTM (L-def), with modified bronchiolar clearance (L-mod1) and also with optimised AI distribution fractions (L-mod2). In addition, alveolar retention for the default HRTM with initial deposition in the alveolar compartments only is shown ($AI/AI_{t=7}$).

t (d)	Exp	L-def	$AI/AI_{t=7}$	L-mod1	L-mod2
50	96 ± 2	76	82	80	95
100	92 ± 4	64	71	70	93
300	78 ± 9	50	57	55	82
900	63 ± 13	31	35	34	60

Table 2. Experimental values (Davis *et al* 2007) for whole body (WB) retention (%) at different times. The mean value (excluding <LLD data) and standard deviation for the seven subjects are shown. The data have been corrected for the effect of radioactive decay (-d) and also absorption (-da). The last two columns show the retention in the lungs and in the AI region as predicted by the HRTM for the insoluble material and inhalation parameters described in the text. All retention values are compared to the retention at seven days after inhalation (100%).

t (d)	WB-d	WB-da	Lungs	$AI/AI_{t=7}$
50	98 ± 17	98 ± 17	76	82
100	82 ± 21	82 ± 21	65	71
300	73 ± 17	73 ± 17	51	57
900	58 ± 19	60 ± 19	31	35
3000	50 ± 10	54 ± 12	9	10
5000	43 ± 10	47 ± 10	6	6

Table 3. Experimental values for lung retention (%) at different times. The mean value (and standard deviation) for the six subjects of the RFP cohort are shown, with correction for the effect of radioactive decay (-d) and also absorption (-da). The last two columns show the retention in the lungs and in the AI region as predicted by the HRTM for the insoluble material and inhalation parameters described in the text. All retention values are compared to retention at seven days after inhalation (100%).

t (d)	Lungs-d	Lungs-da	Lungs	$AI/AI_{t=7}$
50	90 ± 22	90 ± 22	76	81
100	75 ± 23	75 ± 23	65	71
300	53 ± 17	53 ± 18	51	56
900	36 ± 13	36 ± 13	31	34
3000	29 ± 17	30 ± 17	9	10
5000	27 ± 22	27 ± 22	5	6
10000	25 ± 18	26 ± 18	2	3

3. Results

The Philipson *et al* (1996) data are limited to measurements up to 900 days (table 1) and may be used to assess the medium-term clearance, namely for the BB and bb regions and for the short-term alveolar clearance (compartment AI_1 in the HRTM). The Davis *et al* (2007) and the RFP data, which extend to up to 15 and 30 years (tables 2 and 3), are decisive for the analyses of long-term retention, namely, for the distribution fractions and for the transport rates out of the HRTM compartments AI_2 and AI_3 in the HRTM. Changes to the model for the AI region can also be addressed by reconsidering the structure of the linear model as proposed by Kuempel *et al* (2001). The Philipson *et al* (1996) data were examined with both the HRTM and

Kuempel structure for the AI model while the Davis *et al* (2007) and the Rocky Flats Plant data were analysed only with the Kuempel AI model. Because no clear conclusion could be reached about a possible correlation between smoking habit and the slow clearance rates, the results are reported for each cohort as a whole, without distinguishing between smokers and non-smokers.

The HRTM assumes that there is simultaneous absorption to body fluids of material from all the compartments except ET_1. Time-dependent dissolution is represented by a fraction (f_r) that dissolves relatively rapidly, at a rate s_r, and the complementary fraction ($1 - f_r$) that dissolves more slowly, at a rate s_s. (It is usually assumed that uptake of the dissolved material into blood is instantaneous, but there is provision for slower uptake using compartments representing dissolved material 'bound' to respiratory tract tissues.) In the following we will often refer to lung data corrected for decay and absorption to blood:

$$\text{corrected data}(t) = \frac{\text{measured data}(t)}{\exp(-\lambda t)[f_r \exp(-s_r t) + (1 - f_r)\exp(-s_s t)]} \tag{1}$$

where λ is the radioactive decay rate. It is often convenient to look at the corrected data both because the effect of transport clearance is emphasised and because it is possible to set an upper limit to the slow dissolution rate s_s even in the absence of urine data, if lung (or whole body) measurements at sufficiently long times are available. In fact, if the corrected lung data show a clear increasing trend in the long term then the absorption rate s_s has been overestimated or there is an inconsistency between lung and urine data. For an insoluble material, these considerations are also valid when whole body instead of lung measurements are available because there is no significant difference between the whole body and lung retention once the initial fast clearance phase has terminated, a few days after the acute inhalation.

3.1. Philipson et al (1996)

Table 1 shows the mean values of the measured lung retention, as a percentage of the material present seven days after inhalation, for the set of ten subjects. The values were determined here using the reported exponential fits to the lung retention measurements obtained with the NaI detector system. These are higher than those observed in previous studies (ICRP 1994a, 1994b), possibly (at least partly) because of the lower solubility of the material used in this study. The errors shown are the standard deviations for the sample of ten subjects, with the value at $t = 7$ days assumed to be zero. Table 1 also shows the lung retention (L-def) in healthy non-smokers as predicted by the HRTM for an insoluble material ($f_r = 0$ and $s_s = 0\ \text{d}^{-1}$). Deposition in each of the lung compartments, figure 1, was calculated with LUDEP (Jarvis and Birchall 1994) for particle and inhalation parameters specific to the Philipson study. The calculation of deposition requires the breathing rate, the respiratory frequency and the fraction breathed through the nose. Philipson *et al* reported that the aerosol was inhaled at $0.9\ \text{m}^3\ \text{h}^{-1}$. We assumed a low frequency of six breaths per minute, and mouth breathing only. The relative deposition fractions for AI and (BB + bb) are 61% and 39% respectively. Note that the value of $AI/(AI+\text{BB}+\text{bb})$ is not sensitive to variations in the respiratory frequency. Table 1 shows that the retention predicted by the HRTM (L-def) clearly underestimates the experimental results (Exp). The HRTM predicts that seven days after the inhalation, 12% of the remaining material is left in the bronchial tree and 88% in the AI region. After 50 days only about 5% of the deposit at day seven was cleared in the experiment, while the model predicts that 25% would have cleared: 9% from the bronchial tree and 16% from the AI region, each more than that observed. Even assuming that after seven days, 100% of the lung content is in the AI compartments, the observed retention is higher than predicted ($AI/AI_{t=7}$). This indicates an inconsistency between the experimental results and the assumptions in the HRTM model for compartment AI_1: 30% of the AI content clearing with a half-time of 35 days. Additionally,

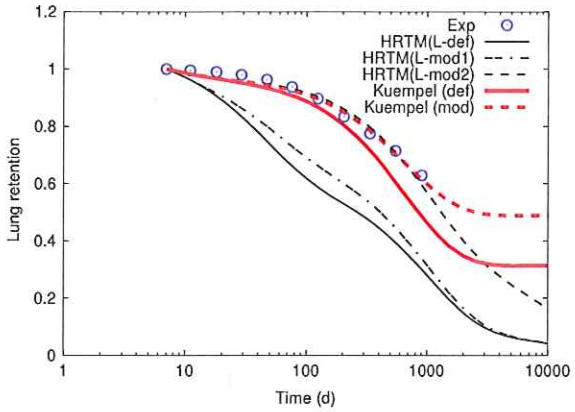

Figure 3. Lung retention from Philipson *et al* data (Exp) and un-weighted LS fit with the HRTM (thin lines) and Kuempel (thick lines) models. The HRTM predictions for the default model (L-def), with modified (Falk model) bronchiolar clearance (L-mod1) and also with optimal alveolar deposition (L-mod2) are shown. The Kuempel model predictions with default (def) and optimised parameters (mod) are shown (modified bronchiolar clearance is also assumed).

even assuming no clearance from the AI region, the HRTM predicts more clearance from the bronchial tree than observed from the lungs here.

To improve the agreement with the measurements, the HRTM was first modified by changes to BB and bb regions (Falk model). The fraction of material left in BB and bb after seven days was then 2% of the lung content at day seven, while the remaining 98% resides in the AI. The difference between the theoretical (L-mod1) and experimental lung retention was reduced but a discrepancy was still evident. To account for the longer retention, the model for the AI region was modified in addition to those for the BB and bb regions. To reduce the lung clearance, the initial distribution between the compartments was varied from the default values, ($a_1 = 0.3$, $a_2 = 0.6$, $a_3 = 0.1$), while the clearance rates were fixed at their default HRTM values. The optimal values for the distribution fractions, obtained with the un-weighted LS method, are ($a_1 = 0$, $a_2 = 0.6$, $a_3 = 0.4$) and the predicted retention (L-mod2) is shown in table 1.

Similarly good results were also obtained with the Kuempel AI model with optimised parameters. As before, a better fit to the data was obtained with the Falk model for the BB and bb regions than with the HRTM. The data from the Philipson study do not allow direct estimation of the sequestered fraction in the AI region because the measurements stopped after 900 days, before any sign of a plateau, but it is plausible to assume that AI_{seq} would eventually have been $\leqslant 0.60$. The optimised parameters are $m = (1.7 \pm 0.3) \times 10^{-3}$ d^{-1} and a strongly correlated ($\rho = 0.96$) value $AI_{seq} = 0.54 \pm 0.05$. Figure 3 shows the experimental data and the predictions of the HRTM and Kuempel *et al* (2001) models with default and optimised parameter values.

Four subjects were non-smokers, three ex-smokers (<28 pack-years) and three smokers (>30 pack-years). The retention at 900 days, with respect to that at day seven, is higher for the smokers ($72 \pm 11\%$), compared to the ex-smokers ($59 \pm 9\%$) and the non-smokers ($59 \pm 11\%$), suggesting slower alveolar clearance rate in the smokers.

Because the Kuempel model provided an adequate fit to these data and is both simpler, and physiologically more realistic than the HRTM, it was adopted in the analyses of both the ^{60}Co and ^{239}Pu data.

3.2. *Davis et al (2007)*

Deposition was calculated using the estimated effective AMAD. Values for individual workers were calculated to be 0.9, 0.3, 0.3, 0.6, 0.4, 0.3 and 0.3 μm. At these sizes the deposition distribution is insensitive to the breathing rate, which implies that the effective AMAD should be a good estimate of the physical AMAD. The mean value for the group of workers was 0.4 μm and a significant fraction, about 40%, of the material deposited in the respiratory tract, would be located in the alveolar region. Table 2 shows the mean value and standard deviation of the measured whole body retention fractions with respect to the value at day seven at different times and for the set of seven subjects. (Because the material was very insoluble, and most cobalt entering the systemic circulation is rapidly excreted in urine, after the first few days whole body retention approximates closely to lung retention.) The data for each subject were linearly interpolated at the selected times and corrected (equation (1)) for the effect of radioactive decay and absorption to blood, with f_r and s_s as estimated with the best fit to each individual's experimental data (table B.1(a)). By comparing the experimental data and the predicted values for an insoluble material (also shown in table 2) it is clear that the HRTM underestimates the lung retention.

In order to obtain good fits to the data it was necessary to modify the default HRTM parameter values, in particular we had to reduce the particle transport clearance of material from the AI region. Each of the seven cases was analysed individually here by using the ICRP systemic model for cobalt (ICRP 1993) and a new lung model obtained by modifying the HRTM. The modifications consisted of the Falk model for the BB and bb regions (although that has little effect because of the low predicted deposition in these regions) and the Kuempel model structure for the AI region. The measurement errors were assumed to be lognormally distributed with scattering factors (approximate geometric standard deviations, which aim to include all sources of error) equal to 1.2, 1.8 and 3, for the whole body, urine and faecal data respectively (Doerfel *et al* 2006).

3.2.1. Parameter and posterior distribution estimates. In order to obtain the best fit to the data, values of the lung absorption parameters f_r and s_s, and the particle transport parameters AI_{seq} and m for the AI region were optimised by fitting the whole body, urine and faecal data for six subjects in the Davis *et al* (2007) study. A seventh case, included in Davis' study, was also analysed but it was not possible to reach any conclusive estimate of the transport parameters (In this case the two parameters AI_{seq} and m are completely correlated, $\rho = 1$, and the sequestration fraction can take any value within the range [0, 1] consistently with the experimental data.) The rapid dissolution rate was kept to its default value, $s_r = 100\ d^{-1}$, the bioassay prediction being insensitive to this parameter because of the low solubility of the material. In Davis *et al* (2007), the fractional uptake of material from the small intestine to the blood, f_l, was estimated to be lower than the default value for cobalt, because of the low urinary excretion. We adopted the same approach by constraining its value to be the same as for the rapid fraction absorbed to blood, $f_l = f_r$. Because the subjects were given a laxative we allowed, as in Davis *et al* (2007), the rates of transit in the GI tract to be larger than the default value up to a factor of 2.5, when this improved the fit to the faecal data.

Each case in the cohort was analysed first by using the maximum-likelihood method with the Levenberg–Marquardt algorithm (ML-LM) method described in section 2.2.3. Results of the parameter optimisation for each subject are shown in appendix B, table B.1. The whole cohort mean values for the sequestered fraction and the clearance rate are $AI_{seq} = 0.4 \pm 0.2$ and $m = 0.002 \pm 0.003\ d^{-1}$. The standard deviations shown give a rough estimate of the large differences in parameter values between subjects. To better estimate the inter-subject variability, the whole cohort PDF (probability distribution function) for each parameter

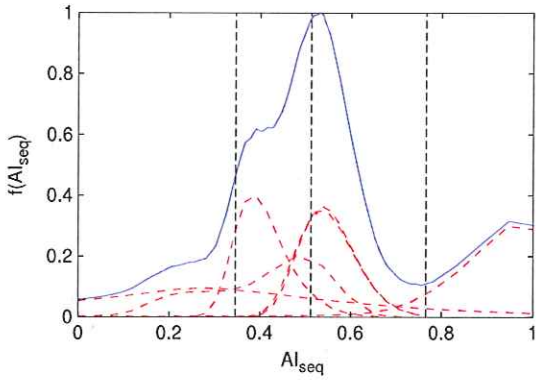

Figure 4. Marginal 1D distribution functions for the estimated transport parameter AI_{seq} from the exact likelihood function for the group of six workers involved in the ^{60}Co incident. The whole cohort marginal distributions (solid line) with peak value normalised to one and the marginal distributions for each of the subjects (dashed lines) are shown. The median value and the 68% central probability interval for the whole cohort are identified by the vertical lines.

was calculated. As described in section 2.2.4, the whole cohort PDF may be obtained by summing each subject's PDF calculated either with the ML-LM method (approximate PDF) or by calculating the exact PDF. Figure 4 shows the exact PDF for the particle transport parameter AI_{seq}, both for the whole cohort and also for each subject. The main statistics of the parameter's PDF are summarised in table B.2(a). The inter-subject variability may be expressed by 68% probability ranges (0.35–0.76) for AI_{seq} and (0.0006–0.01) d^{-1} for m. The exact PDFs for the two transport parameters can be approximated by two lognormal distributions $AI_{seq} \sim LN(0.5, 1.5)$ and $m \sim LN(0.003, 4)$.

Three of the subjects were non-smokers (cases 4–6) and three were smokers (cases 1–3; cigarettes smoked: 10, 20, 20 per day). The transfer rate m was, on average, lower in the smokers and this leads to higher retention in the first years. On the other hand, the sequestered fraction is higher in non-smokers and this implies that the retention is higher for the non-smokers in the long term. The relatively small number of cases analysed does not allow a definitive conclusion about the effects of smoking on lung retention.

3.3. Rocky Flats Plant

Table 3 shows mean values and standard deviations of the measured lung retention fractions at different times with respect to the value at day seven for the set of six subjects. The values were obtained with the same procedure as for the cobalt cases (section 3.2) except that for three cases extrapolation at early times also had to be used. Note that the corrections for the effects of both radioactive decay and absorption are very small. The long-term trend in the lung measurements (Lungs-d) is a clear indication that both clearance mechanisms, particle transport and absorption, are very weak. The overall clearance rate can be roughly estimated to be of the order of 10^{-5} d^{-1} or less for all cases and may be considered an upper limit for both the slowest AI transport rate and the slow absorption rate to blood. This suggests that the slowest transport rate for the lungs should at least be reduced by a factor of 10 in the HRTM. For the Kuempel model, where a fraction of the deposited material is sequestered in the lungs (and lymph nodes), the long-term trend in the lung measurements implies a value of the order of 10^{-5} d^{-1} for the slow dissolution rate s_s for this material. A rough estimate of the fraction of material sequestered in the interstitium is $AI_{seq} = 20$–30%.

Each of the six RFP cases contaminated in the 1965 fire accident was analysed individually following the same procedure as for the cobalt cases described in section 3.2. The rapid dissolution rate was kept to its default value, $s_r = 100\ d^{-1}$, because its value has little effect on the estimated long-term clearance rates. The possible existence of a bound state for plutonium (ICRP 2002, Khokhryakov *et al* 2005, James *et al* 2007) was neglected in this analysis, for simplicity. Since the material appears to be of very low solubility it is likely that very little of the plutonium in the lungs had the potential to be in the 'bound state' compartments.

3.3.1. Parameter and posterior distribution estimates. The analysis follows the same steps as for the cobalt cohort. The results of the ML-LM optimisation for each subject are shown in table B.1(b). The sequestered fraction was confirmed to indicate longer retention than the HRTM predicts but the whole cohort mean value of $AI_{seq} = 0.3$ was lower than for the cobalt cohort. Differences in parameter values between subjects were also significant within this cohort. The analysis of the whole cohort exact PDF (results are summarised in table B.2(b)) shows that the 68% probability ranges representing the inter-subject variability are (0.19–0.65) for AI_{seq} and (0.0008–0.065) d^{-1} for m. The whole cohort exact PDFs may be approximated by two lognormal distributions: $AI_{seq} \sim LN(0.27, 1.6)$ and $m \sim LN(0.0023, 3)$. Uncertainties in the content of ^{241}Am and ^{241}Pu in the inhaled aerosol may affect the estimates of the lung clearance parameters. For instance, over(under)estimates of about 50% in either of the two concentrations would results in under(over)estimates of the sequestered fraction of about 25%.

Based on the information about the smoking habits of the subjects (subjects 2 and 3 are non-smokers; 4 is a heavy smoker; 1, 5 and 6 are ex-smokers, 0.5–1 pack/day for different periods), no correlation was found with the estimated particle transport parameters.

The additional three RFP cases included in the NIOSH report (ORAUT 2007), not part of the set of six cases involved in the same incident analysed here, also show longer lung retention for insoluble plutonium than the HRTM predicts and the estimated values for the particle transport parameters are close to those obtained above for the other RFP cases. The mean value for the three ML estimates are $AI_{seq} = 0.25 \pm 0.04$ and $m = 0.0011 \pm 0.0003\ d^{-1}$.

3.4. Analysis of complete dataset

In this section the cobalt and plutonium results are merged and analysed first and then the Philipson *et al* (1996) data and the results which were the basis for the present HRTM are included to estimate the best values for the particle transport clearance parameters for the new AI model. To complete the model description the particle transport rate to the lymph nodes is also determined.

3.4.1. Analysis of the cobalt-60 and Rocky Flats Plant cases. We report here only the results obtained by merging the exact parameter posterior distributions of the 12 ^{60}Co and RFP subjects. The most important information extracted from these two datasets is the estimates of the sequestered fraction and of the inter-subject variability for all four transport parameters. The Philipson and previous experiments on which the HRTM is based are unlikely to influence the estimate of AI_{seq} but they will play a role in the estimation of the clearance rate m which is determined mostly by data in the range 100–1000 days. Figures 5(a) and (b) show the posterior distribution for AI_{seq} and m and the approximating lognormal distribution obtained by fitting the corresponding cumulative posterior. Median values are $AI_{seq} = 0.39$ and $m = 0.003\ d^{-1}$. The distributions for the model parameters m_I and m_T, shown in figures 5(c) and (d), are obtained by using random sampling from the joint posterior distribution of AI_{seq} and m. Median values are $m_T = 0.0012\ d^{-1}$ and $m_I = 0.0011\ d^{-1}$. The 68% central probability intervals

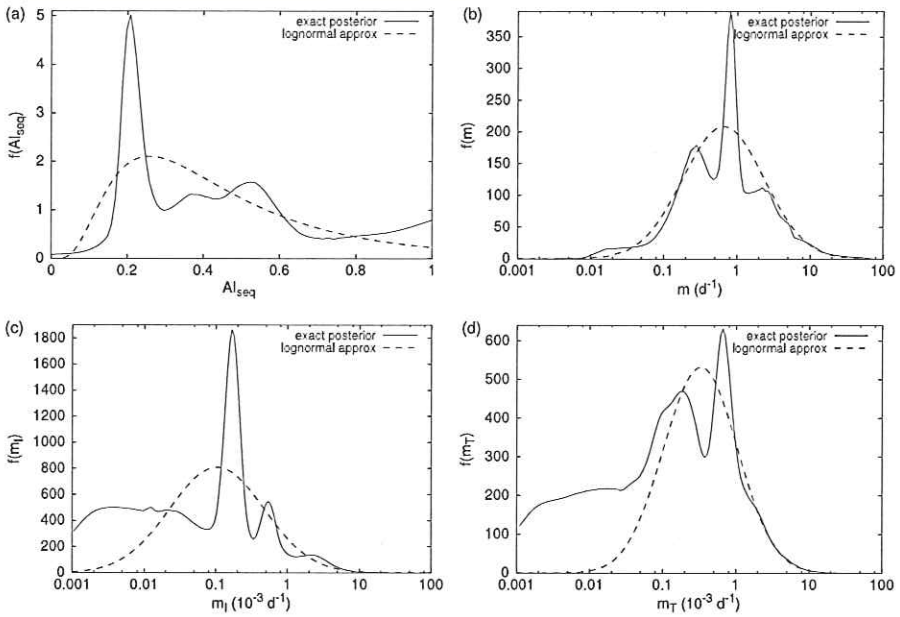

Figure 5. Marginal 1D distribution functions for the estimated transport parameters AI_{seq} (a), m (b), m_{I} (c) and m_{T} (d) for the Co-60 and RFP cohorts. The whole cohort marginal distribution (solid) is calculated from the exact posterior and its lognormal approximation (dashed).

representing inter-subject variability for these parameters are given in table 4. The geometric standard deviations of the approximating lognormal distribution (table 4) is an alternative way, and here only approximate, to define the same interval. Note that even though the correlation between AI_{seq} and m resulting from the fitting procedure was significant in many subjects, the correlation coefficient is low, $\rho = 0.26$, when calculated with the whole ^{60}Co and RFP cohort distribution.

3.4.2. Analysis of 'new' and ICRP Publication 66 data. The parameters for the new AI model were estimated from a dataset which includes data presented in the previous sections plus data reported in annex E of ICRP (1994a) and based on experimental work by Jammet *et al* (1978), Bohning *et al* (1982) and Bailey *et al* (1985).

In order to use the different datasets in the fitting procedure consistently, we assumed that after seven days there is only material left in the AI region. To produce a representative set of points for both the ^{60}Co and RFP cohorts a few transformations of the data were required. Data for each subject were first corrected for the effects of radioactive decay and absorption and normalised to the value at day seven. The values for the absorption parameters that were estimated in the previous sections are given in table B.1. In a few of the cases, the value at day seven had to be extrapolated because there were no early data. The data were then interpolated to the same set of time points and finally averaged with the same weight for each cohort. Values were computed at $t = 50,\ 100,\ 300,\ 900$ for consistency with the other datasets (ICRP 1994a, 1994b) and Philipson *et al* 1996 and from $t = 2000$ onwards with time steps of 1000 days.

All the datasets are shown in figure 6 together with the predictions of the HRTM and Kuempel *et al* (2001) models with default parameters. An un-weighted least squares fit to

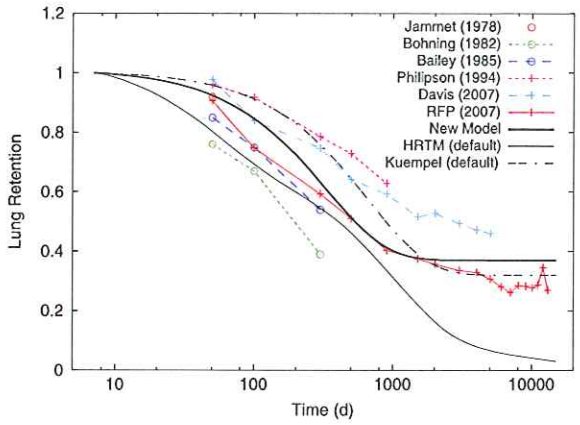

Figure 6. Measured lung retention data (Philipson *et al* (1996), Davis *et al* (2007), RFP (ORAUT 2007) studies and studies reported in annex E, ICRP 1994a) are shown together with the model predictions by assuming initial deposition in the alveolar region only. Predictions of both the HRTM and Kuempel *et al* (2001) model with default parameter values are shown. The 'New Model' curve was obtained with optimised AI particle transport parameters $AI_{seq} = 0.37$ and $m = 0.0027\ d^{-1}$.

Table 4. Best fit (for averaged data) values and inter-subject variability for the particle transport parameters AI_{seq}, m, m_I and m_T. Central 68% probability intervals (inter-subject variability) are calculated from the exact posterior of the merged ^{60}Co-RFP cohort. $LN(-, -)$ indicate the approximating lognormal distribution.

		Inter-subject variability	
	Best fit	68% probab. interval	Distribution
AI_{seq}	0.37	0.2–0.7	$LN(0.38, 1.9)$
m (10^{-3} d^{-1})	2.7	0.8–9	$LN(2.6, 3.4)$
m_I (10^{-3} d^{-1})	1.0	0.2–4	$LN(1.0, 4.5)$
m_T (10^{-3} d^{-1})	1.7	0.4–4	$LN(1.3, 3.2)$

the experimental retention data using the new AI model gave the optimised parameter values $AI_{seq} = 0.37$ for the sequestered fraction and $m = 0.0027\ d^{-1}$ (half-time of about 250 days) for the clearance rate from the alveolar compartment. In this case, the parameter covariance matrix and the complete likelihood function in the two-dimensional parameter space give almost exactly the same answer: the uncertainty on the best fit parameter values is described by a normal distribution $N(0.37, 0.025)$ for AI_{seq} and a lognormal distribution $LN(0.0027, 1.2)$ for m. Note that the error given is the uncertainty on the best fit value and is much smaller than the inter-subject variability for the cohorts we have analysed. It was also found that the best fit parameters are correlated with a correlation coefficient $\rho = 0.5$.

Equivalently, the best estimates for the transfer rates from the alveolar compartment to the interstitium and to the bronchiolar region to be used in the new model are $m_I = 0.0010\ d^{-1}$ and $m_T = 0.0017\ d^{-1}$, respectively. The uncertainty on the best estimates of these parameters is represented by two lognormal distributions: $m_I \sim LN(0.001, 1.3)$ and $m_T \sim LN(0.0017, 1.2)$ and the correlation coefficient is $\rho = 0.9$.

The values for the transport parameters AI_{seq} and m here estimated as best fit value for the averaged data are very close to the values obtained previously as median values for the set of 12 subjects of the merged ^{60}Co and RFP cohort. Table 4 summarises the results for both the

best parameter values obtained from fitting the averaged data (each cohort is represented by the average retention data) and the inter-subject variability. The latter is based on the information from each subjects analysis for the merged ^{60}Co and RFP cohorts. Both the 68% central probability interval and the approximating lognormal distribution which best fits the cumulative distribution are given.

3.5. Clearance to thoracic lymph nodes

In the HRTM the transport rate from the AI region to the thoracic lymph nodes, $m_{\mathrm{AI-LN}} = 2 \times 10^{-5}$ d^{-1}, was determined to give the ratio of material concentration in lymph nodes and lungs equal to the value estimated from autopsy data: for non-smokers $[LN]/[L] \approx 20$ after 10 000 days (Kathren *et al* 1993).

Because of the longer AI retention in the new model, the amount cleared to the lymph nodes from the airway walls (BB_{seq} and bb_{seq}) is now negligible compared to that from the AI region. The same value for $[LN]/[L]$ is obtained either with or without considering clearance from the BB_{seq} and bb_{seq} compartments. The ratio $[LN]/[L] \approx 20$ is obtained with the value $m_{\mathrm{AI-LN}} = 3 \times 10^{-5}$ d^{-1} for the transport rate from the alveolar interstitium to the thoracic lymph nodes.

4. Discussion

The measurements analysed here show a clear inconsistency with the long-term retention in the lungs predicted by the HRTM. The data could be represented by modifying the parameter values of the HRTM without changing its structure (as done in Davis *et al* (2007) for the ^{60}Co cases), but the predictions of the proposed new AI model are equally consistent. In the latter, the material is deposited in the alveolar compartment, and transfers to the bronchiolar region and to the interstitium at rates $m_{\mathrm{A-bb}} = m_{\mathrm{T}} = 0.0017$ d^{-1} and $m_{\mathrm{A-I}} = m_{\mathrm{I}} = 0.0010$ d^{-1}. The observed lung retention can be represented by the HRTM by modifying its parameter values but without changing its structure: $AI = (0, 0.63, 0.37)$ for the initial distribution and $m_{\mathrm{AI1-bb}} = m_{\mathrm{AI3-bb}} = 0$ and $m_{\mathrm{AI2-bb}} = 0.0027$ d^{-1}, i.e., without introducing transfer of material between AI compartments (this alternative formulation is used in the next section for the calculation of the dose to the lung). The predictions for retention in lung plus lymph nodes are exactly the same for the two models while the predicted ratio of lymph nodes to lung concentration as a function of time differs only slightly. The two values can be made equal only at one arbitrarily fixed time point (for instance at 10 000 days). With $m_{\mathrm{AI-LN}} = 3 \times 10^{-5}$ d^{-1}, the two different formulations give, in any case, very similar values for $[LN]/[L]$, 22 and 23 for the Kuempel and the modified HRTM model respectively, well within the experimental uncertainty. However, compared to the HRTM, the Kuempel model is biologically more realistic in representing the clearance of insoluble particles in the human lungs and simpler (only two instead of three compartments for the AI region and only two instead of five parameters to be defined). Clearance mechanisms from the AI region are complex and not completely understood (ICRP 1994a). A list, which includes alveolar macrophages (AM)-mediated transport and free-particle transport on and through the alveolar epithelium, is given by Kreyling and Scheuch (2000). However, it is recognised that the most important clearance pathways, as assumed by Kuempel *et al* (2001), are transport mediated by alveolar macrophages toward the ciliated airways and transport to the interstitium for the remaining particles. Particles that reach the ciliated airways will gain access to the mucociliary escalator and be removed from the body via the GI tract, while the remaining particles are translocated within the lungs into the interstitial spaces and eventually transported to the regional lymph nodes.

There is also evidence (Kreyling and Scheuch 2000) that phagocytosis by AM is more active for particle diameters in the range 0.5–2 μm, whereas smaller particles can be directly interstitialised (free-particle transport). For both the ^{60}Co and the PuO_2 cases the inhaled aerosols are characterised by a relatively small mass median diameter of 0.3 μm. (For the PuO_2, the measured mass median diameter was 0.32 μm (section 2.1). For the ^{60}Co, the AMAD was estimated to be 0.4 μm (section 3.2). Assuming ICRP default aerosol values for particle density and shape factor, $\rho_m = 3$ g cm^{-3} and $\chi = 1.5$ respectively, the average mass median diameter is $d = d_{ae}\sqrt{\chi/\rho_m} = 0.3$ μm). The HRTM deposition model predicts in both cases that about 30% of the mass deposited in the AI region is carried by particles with diameter in the range 0.5–2 μm, the rest being carried by smaller particles. However, for the coal miners studied by Kuempel and co-workers, it was assumed that the particles had both physical and aerodynamic diameter of about 5 μm (with $\sigma_G = 2.5$). In this case, about 60% of the mass deposited in the AI region is carried by particles with diameter in the range 0.5–2 μm and the remainder by larger particles. Based on this information and on the values estimated here for the particle transport rates we could not find a correlation between the rate of interstitialisation and the particle size. Despite the different sizes of the inhaled particles, all the aforementioned analysis and studies agree in predicting that about 30%–40% of the material deposited in the AI region remains sequestered indefinitely, i.e., have reached the interstitial region in one way or another.

The three groups of subjects studied here included current smokers, and non-smokers, and two groups included ex-smokers. However, because of the degree of inter-subject variation, and the small numbers in each group, no clear conclusions could be drawn about the effect, if any of smoking on long-term lung retention of insoluble particles. In all of the experimental human lung studies reviewed in ICRP Publication 66 (ICRP 1994a) in which smokers and non-smokers were compared, retention was greater in smokers. On that basis modifying factors were proposed to reduce transfer rates from the AI region to the bronchiolar region in smokers (the HRTM default parameter values were intended to apply to healthy non-smokers). It was noted that the difference was most marked in studies in which retention of ferromagnetic iron oxide particles was measured by magnetopneumography (MPG). Since the retention half-times measured in non-smokers in these studies were considerably shorter than in studies using more inert particles (e.g. Teflon), it was inferred that dissolution was an important mechanism in clearance of the iron oxide particles, and that it was reduced in smokers. This is supported by more recent studies. In particular, Möller *et al* (2001) measured retention up to 300 days after inhalation of ferromagnetic iron oxide particles. For healthy subjects, the half-time of the slow phase of lung clearance was shorter in non-smokers than in smokers: in younger subjects (20–39 years) 124 ± 66 d versus 220 ± 74 d and in older subjects (40–65 years) 162 ± 120 d versus 459 ± 334 d. It is possible that smoking has a greater effect on alveolar clearance in the first few months than at later times, or that dissolution made a significant contribution to clearance in all the studies reviewed by ICRP (1994a) which compared smokers and non-smokers.

4.1. Dose assessments

The new AI model predicts longer lung retention compared to the HRTM and this will potentially result in higher doses to the lungs. Table 5 shows the equivalent dose to the lungs and the effective dose for a unit intake (Bq) for a few radionuclides in their insoluble form (absorption type S) and for an AMAD of 5 μm. The doses for more soluble forms (type M and F) are not affected by the longer lung retention. The doses were calculated using IMBA (Birchall *et al* 2007) for the HRTM with default parameter values and with the new lung model in its 'equivalent' form (figure 2(b)), where the HRTM structure is kept, the Falk model and the optimised AI clearance parameter values are used: $AI = (0.63, 0.37)$ for the initial distribution

Table 5. Equivalent dose to the lungs (μSv) and effective dose (μSv) per unit intake (Bq) of the given radionuclide. Values were calculated with the default HRTM model ($a_1 = 0.3$, $a_2 = 0.6$, $a_3 = 0.1$) and the new lung model ($AI_{seq} = 0.37$, $m = 0.0027$ d^{-1}).

	Lung equivalent dose coefficient (μSv Bq^{-1})		Effective dose coefficient (μSv Bq^{-1})	
	HRTM	New model	HRTM	New model
U-238	34	60	6	9
Pu-239	47	75	8	16
Am-241	52	79	9	15
Co-60	0.10	0.12	0.016	0.021

and $m = 0.0027$ d^{-1}. With this new model, the equivalent dose to the lungs increases by a factor of about 1.5–2 for insoluble long-lived alpha-emitting radionuclides and by about 20% for ^{60}Co (the same result would be obtained with the Kuempel model structure for AI). By keeping the fast clearance phase only for the bronchial region (Falk model) the lung dose is reduced and this partially cancels the increase due to the longer retention in the AI region.

5. Conclusions

Since the adoption of the HRTM, four studies (Philipson *et al* (1996), Kuempel *et al* (2001), Davis *et al* (2007) and ORAUT (2007)) have been reported which provide more comprehensive information for long-term lung retention than was available when the HRTM was developed. All four studies show that the HRTM underestimates long-term retention.

The model of Kuempel *et al* (2001) provides a physiologically more realistic and simpler model of *AI* retention than the HRTM, and was shown to provide an adequate representation of *AI* retention for the data in the other three studies. A new model was developed here, taking the Kuempel *et al* (2001) model structure but fitting both to experimental datasets on which the HRTM parameter values were based, and to the more recent, long-term studies analysed here. About 40% of an insoluble material deposited in the AI region remains sequestered indefinitely and slowly clears only to the lymph nodes. The remaining material is cleared with half-time of about 300 days.

Due to the increased retention, the lung dose per unit intake for insoluble long-lived alpha-emitting radionuclides increases by 50–100%. The relatively small number of subjects analysed did not allow identification of a clear effect of smoking on the long-term retention.

The new AI model structure is shown in figure 2(a) and the values for the particle transport rates are $m_I = 0.001$ d^{-1} from the alveolar compartment to the interstitium, and $m_T = 0.0017$ d^{-1} from the alveolar compartment to the bronchiolar region. The inter-subject variability is here quantified with the 68% central probability intervals: $(0.2, 4) \times 10^{-3}$ d^{-1} for m_I and $(0.4, 4) \times 10^{-3}$ d^{-1} for m_T. For uncertainty analysis, a reasonably accurate representation of the parameter distributions is given by two uncorrelated lognormal distributions: $m_I \sim LN(0.001, 4)$ and $m_T \sim LN(0.0017, 3)$ or, for the alternative formulation, by $AI_{seq} \sim LN(0.37, 2)$ and $m \sim LN(0.0027, 3)$.

Acknowledgments

We thank NIOSH for providing the data for the Rocky Flats Plant workers used in this study. We are especially grateful to Professor Joyce Lipsztein for drawing our attention to the existence of the long-term follow up measurements on these workers and for the help in obtaining permission to use them here.

Appendix A. Maximum-likelihood for data below LLD

Tobin (1958) has shown that in presence of left censored data, an appropriate likelihood function which possesses desirable properties (consistency, efficiency) is the following, also known as Tobit (Tobin probit) likelihood function (Amemiya 1984):

$$L(x;\theta) = \prod_{i=1}^{n_+} \mathrm{PDF}(x_i;\theta) \prod_{i=1}^{n_-} \mathrm{CDF}(x_{i0};\theta)$$

where n_- and n_+ are the number of measurements below and above the lower limit of detection (LLD) x_{j0}, PDF and CDF are the probability density function and the cumulative density function respectively, for the random variable x and distribution parameters θ. The maximum-likelihood estimator for the intake I in case of normal errors is obtained by maximising the log-likelihood $\log(L(x;\theta))$ or, equivalently, by minimising

$$\sum_{i=1}^{n_+} \left[\left(\frac{x_i - Im_i}{\sigma_i} \right)^2 \right] - 2 \sum_{i=1}^{n_-} \log \left\{ \frac{1}{2} \left(1 + \mathrm{erf} \left[\frac{x_{i0} - Im_i}{\sigma_i \sqrt{2}} \right] \right) \right\}$$

where m_i is the model prediction for unit intake, σ_i is the assumed error on the measurement and $\mathrm{erf}(\cdot)$ is the error function. Note that once the intake has been estimated, $I \rightarrow \hat{I}$, the importance, or weight, of a <LLD data point in the maximisation can be represented with an 'equivalent χ^2' defined as

$$\chi^2_{\mathrm{equiv}} = -2 \log \left\{ \frac{1}{2} \left(1 + \mathrm{erf} \left[\frac{x_0 - \hat{I}m}{\sigma \sqrt{2}} \right] \right) \right\}.$$

Appendix B. Methods and results

B.1. Maximum-likelihood Levenberg–Marquardt method

The ML-LM optimisation procedure to determine the model parameters for each subject may be summarised as follows. Starting with an initial guess $\boldsymbol{p}_0$ for the parameters, for each step of the iteration, until the maximum of the likelihood function is achieved in the parameter space: (1) the first-order kinetics lung + biokinetic model is solved with given values for the parameters and the time-series of *in vivo* and bioassay predictions are computed for a unit intake; (2) the intake is calculated using the maximum-likelihood method by comparing the model prediction and the measurements; (3) the parameters are changed according to the LM algorithm, which is searching for a local maximum $\boldsymbol{p}_{\max}$ of the log-likelihood function in parameter space. The software GNU-Octave (Eaton 2002) was used to implement numerically the optimisation procedure, here, for the parameters f_{r}, s_{s}, AI_{seq} and m. The estimated parameter covariance matrix obtained with the above ML-LM optimisation contains the information for a normal approximation of the N-dimensional likelihood function $L(\boldsymbol{p})$ in the neighbourhood of $\boldsymbol{p}_{\max}$. The result of the optimisation can therefore be summarised with a multivariate normal-likelihood function $N(\boldsymbol{p};\boldsymbol{\mu}_p,\boldsymbol{\Sigma}_p|\boldsymbol{x})$ for each subject, eventually truncated for bounded parameters (for instance, $0 \leqslant AI_{\mathrm{seq}} \leqslant 1$).

Two parameters, f_{r} and m, have been transformed for the optimisation ($p \rightarrow \log(p)$) and the corresponding uncertainties are shown as a geometric standard deviation (the symbol '$\cdot/$' is used). The parameter s_{s} was optimised, as AI_{seq}, without being transformed and the uncertainty is shown as an arithmetic standard deviation (the symbol $\pm$ is used). Table B.1 shows the results of the parameter optimisation obtained with the ML-LM method for each subject of the ^{60}Co and RFP cohorts respectively. The 'equivalent' χ^2, shown in brackets, quantifies the contribution of the <LLD data to the likelihood function (appendix A).

Table B.1. Parameter values used to fit the whole body, urine and faecal data for six subjects in the ^{60}Co study (a) and parameter values used to fit the lung and urine data for the six RFP cases contaminated in the 1965 fire accident (b). The standard errors on the parameter estimates (shown in brackets) were evaluated from the parameter covariance matrix obtained with the ML-LM method. The number of data, both measured and <LLD (in brackets), and their corresponding contribution to the χ^2 value (the equivalent value for the <LLD data points in brackets) are shown in the last two columns.

(a) ^{60}Co cohort

Case	$f_t = f_1(10^{-3})$	$s_s(10^{-5}\ d^{-1})$	AI_{seq}	$m\ (10^{-3}\ d^{-1})$	No. data	χ^2
1	0.7(·/1.3)	0(±2)	0.32(±0.04)	1.1(·/1.3)	39(2)	31(1)
2	1.4(·/1.6)	6(±6)	0.0(±0.6)	0.2(·/3)	32(4)	42(5)
3	1.2(·/1.7)	14(±7)	0.20(±0.06)	1.6(·/1.3)	25(5)	26(8)
4	1.1(·/1.3)	0(±2)	0.6(±0.2)	0.4(·/3)	40(5)	35(1)
5	1.5(·/1.3)	0(±2)	0.49(±0.05)	7(·/1.4)	32(3)	18(1)
6	1.8(·/1.3)	0(±2)	0.52(±0.06)	3(·/1.5)	29(2)	23(0)

(b) RFP cohort

Case	$f_t\ (10^{-3})$	$s_s\ (10^{-5}\ d^{-1})$	AI_{seq}	$m\ (10^{-3}\ d^{-1})$	No. data	χ^2
1	5(·/1.7)	0.3(±1.1)	0.22(±0.07)	11(·/1.5)	60	67
2	8(·/1.4)	0.0(±0.2)	0.11(±0.02)	5(·/1.2)	99	47
3	3(·/3)	0.46(±0.13)	0.34(±0.12)	3(·/2)	27(2)	32(7)
4	80(·/1.8)	0.0(±0.7)	0.71(±0.09)	6(·/3)	76	31
5	0.5(±4)	3(·/1.2)	0.20(±0.012)	0.8(·/1.1)	138	66
6	7(·/1.3)	0.4(±0.1)	0.22(±0.02)	0.8(·/1.3)	108	59

B.2. Posterior distribution calculation

Non-informative (uniform) prior distributions were assumed for the parameters (in the range of values where the parameter are defined) and the posterior distribution is therefore numerically equal to the likelihood function with the constraint that its integral on the parameter space is equal to one. Only in one case the upper limit for the transport parameter m was not well defined. The likelihood function did anyway show a clear maximum. A prior distribution was therefore included to limit the values of m to be not larger than those for the transport rates in the bronchiolar region.

The whole cohort PDF was obtained by summing each subject's PDF. The marginal one-dimensional PDF for each of the parameters were then obtained by integration. These parameter distributions are described in terms of a set of quantiles and can be tentatively approximated with a normal/lognormal distribution (see table B.2). The subject's PDF were determined either by using the multinormal approximation provided by the ML-LM method (approximate posterior) or by calculating the likelihood function on a Cartesian grid in the 4D parameter space (exact posterior) using the information provided by the ML-LM method to speed up the mapping. The ML-LM optimisation procedure, in fact, provides the maximum and a reasonable estimation of the region in parameter space where the likelihood function is more important and, in this way, it is possible to avoid calculating the likelihood function where its value is negligible. This still required computing the likelihood function about 5×10^4 times on a grid with 20 points per dimension to define the 95% probability region. The multinormal approximation to the parameters posterior obtained with the ML-LM method was reasonably good for most of the ^{60}Co and RFP cases analysed. Differences between the approximate and exact posterior were significant mainly in regions of the parameter space where the likelihood was small. In general, the ML-LM procedure is very valuable for a rapid assessment and provides guidance for calculating the exact posterior.

Table B.2. Quantiles are shown for each of the parameter marginal (1D) probability distributions obtained from the exact posterior. The column '$LN(\mu, \sigma)$' shows the median and the geometric standard deviation of the approximating lognormal (LN) distribution.

	2.5%	16%	50%	84%	97.5%	$LN(\mu, \sigma)$	
(a) ^{60}Co cohort							
f_r (10^{-3} d^{-1})	0.4	0.7	1.2	2	3	1.1	1.7
s_s (10^{-5} d^{-1})	0.2	1.4	5	20	40	5	4
AI_{seq}	0.12	0.35	0.51	0.76	0.97	0.50	1.5
m (10^{-3} d^{-1})	0.2	0.6	3	10	20	3	4
(b) RFP cohort							
f_r (10^{-3} d^{-1})	0.5	1.9	5	30	60	5	4
s_s (10^{-5} d^{-1})	0.04	0.18	0.4	1.7	3	0.4	2
AI_{seq}	0.16	0.19	0.23	0.65	0.91	0.27	1.6
m (10^{-3} d^{-1})	0.6	0.8	3	7	17	2	3

Table B.2 shows the main statistics calculated from the exact PDF for each of the optimised parameters for the whole ^{60}Co and RFP cohorts respectively. The columns '$LN(\mu, \sigma)$' show the characteristic parameters of the best-fitting lognormal distribution to each PDF.

References

Amemiya T 1984 Tobit models: a survey *J. Econometr.* **24** 3–61

Bailey M R, Ansoborlo E, Guilmette R A and Paquet F 2007 Updating the ICRP human respiratory tract model *Radiat. Prot. Dosim.* **127** 31–4

Bailey M R, Fry F A and James A C 1985 Long term retention of particles in the human respiratory tract *J. Aerosol Sci.* **16** 295–305

Bailey M R, Harrison J D, Jones K A, Marsh J W and Prosser S L 1997 Uncertainties in aspects of internal dosimetry relevant to accident consequence assessment codes *NRPB-M763* (Chilton: NRPB)

Birchall A, Puncher M, Marsh J W, Davis K, Bailey M R, Jarvis N S, Peach A D, Dorrian M D and James A C 2007 IMBA professional plus: a flexible approach to internal dosimetry *Radiat. Prot. Dosim.* **125** 194–7

Bohning D E, Atkins H L and Cohn S H 1982 Long-term particle clearance in man: normal and inpaired *Ann. Occup. Hyg.* **26** 259–71

Davis K, Marsh J W, Gerondal M, Bailey M R and Le Guen B 2007 Assessment of intakes and doses to workers followed for 15 years after accidental inhalation of ^{60}Co *Health Phys.* **92** 332–44

Doerfel H *et al* 2006 General guidelines for the estimation of committed effective dose from incorporation monitoring data *Research Report FZKA 7243* (Karlsruhe: Research Center Karlsruhe) available at http://bibliothek.fzk.de/zb/berichte/FZKA7243.pdf accessed 21 May 2010

Draper N R and Smith H 1998 *Applied Regression Analysis* (New York: Wiley)

Eaton J W, Bateman D and Hauberg S 2008 *GNU Octave Manual Version 3* (Godalming: Network Theory Limited) ISBN: 0-9546120-6-X http://www.octave.org

Falk R, Philipson K, Svartengren M, Bergman R, Hofmann W, Jarvis N, Bailey M and Camner P 1999 Assessment of long-term bronchiolar clearance of particles from measurements of lung retention and theoretical estimates of regional deposition *Exp. Lung Res.* **25** 495–516

Fell T, Phipps A W and Smith T J 2007 The internal dosimetry code PLEIADES *Radiat. Prot. Dosim.* **124** 327–38

Hurtgen C *et al* 2007 IDEAS internal contamination database: a compilation of published internal contamination cases. A tool for the internal dosimetry community *Radiat. Prot. Dosim.* **125** 520–2

ICRP 1993 Age-dependent doses to members of the public from intake of radionuclides: part 2 ingestion dose coefficients *ICRP Publication 67; Ann. ICRP* **23** (3–4)

ICRP 1994a Human respiratory tract model for radiological protection *ICRP Publication 66; Ann. ICRP* **24** (1–3)

ICRP 1994b Dose coefficients for intakes of radionuclides by workers *ICRP Publication 68; Ann. ICRP* **24** (4)

ICRP 1995 Age-dependent doses to members of the public from intake of radionuclides: part 4 inhalation dose coefficients *ICRP Publication 71; Ann. ICRP* **25** (3–4)

ICRP 1996 Age-dependent doses to members of the public from intake of radionuclides: part 5 compilation of ingestion and inhalation dose coefficients *ICRP Publication 72*; *Ann. ICRP* **26** (1)

ICRP 1997 Individual monitoring for internal exposure of workers: replacement of ICRP Publication 54 *ICRP Publication 78; Ann. ICRP* **27** (3–4)

ICRP 2002 ICRP supporting guidance 3: guide for the practical application of the ICRP human respiratory tract model *Ann. ICRP* **32** (1–2)

James A C, Sasser L B, Stuit D B, Glover S E and Carbaugh E H 2007 USTUR whole body case 0269: demonstrating effectiveness of i.v. Ca-DTPA for Pu *Radiat. Prot. Dosim.* **127** 449–55

Jammet H, Drutel P, Parrot R and Roy M 1978 Étude de l'épuration pulmonaire chez l'homme après administration d'aérosols de particules radioactives *Radioprotect. DUNOD* **13** 143–66

Jarvis N S and Birchall A 1994 LUDEP 1.0, a personal computer program to implement the new ICRP respiratory tract model *Radiat. Prot. Dosim.* **53** 191–3

Kathren R L, Strom D J, Sanders C L, Filipy R E, McInroy J F and Bistline R E 1993 Distribution of plutonium and americium in human lungs and lymph nodes and relationship to smoking status *Radiat. Prot. Dosim.* **48** 307–15

Khokhryakov V F, Suslova K G, Vostrotin V V, Romanov S A, Eckerman K F, Krahenbuhl M P and Miller S C 2005 Adaptation of the ICRP Publication 66 respiratory tract model to data on plutonium biokinetics for Mayak workers *Health Phys.* **88** 125–32

Kreyling W G and Scheuch G 2000 Clearance of particles deposited in the lungs *Particle–Lung Interactions* ed P Gehr and J Heyder (New York: Dekker) pp 323–76

Kuempel E D, O'Flaherty E J, Stayner L T, Smith R J, Green F H and Vallyathan V 2001 A biomathematical model of particle clearance and retention in the lungs of coal miners *Regul. Toxicol. Pharmacol.* **34** 69–87

Kuempel E D and Tran C L 2002 Comparison of human lung dosimetry models: implications for risk assessment *Ann. Occup. Hyg.* **46** 337–41

Leggett R W, Eckerman K F, Khokhryakov V F, Suslova K G, Krahenbuhl M P and Miller S C 2005 Mayak worker study: an improved biokinetic model for reconstructing doses from internally deposited plutonium *Radiat. Res.* **164** 111–22

Mann J R and Kirchner R A 1967 Evaluation of lung burden folllowing acute inhalation exposure to highly insoluble PuO_2 *Health Phys.* **13** 877–82

Marsh J W *et al* 2008 Internal dose assessments: uncertainty studies and update of IDEAS guidelines and databases within CONRAD project *Radiat. Prot. Dosim.* **131** 34–9

Miller G, Martz H F, Little T T and Guilmette R 2002 Bayesian internal dosimetry calculations using Markov chain Monte Carlo *Radiat. Prot. Dosim.* **98** 191–7

Möller W, Barth W, Kohlhäufl M, Häussinger K, Stahlhofen W and Heyder J 2001 Human alveolar long-term clearance of ferromagnetic iron oxide microparticles in healthy and diseased subjects *Exp. Lung Res.* **27** 547–68

ORAUT (Oak Ridge Associated Universities Team) 2007 Estimating doses for plutonium strongly retained in the Lung Rev 00 February 6 *ORAUT–OTIB–0049*

Philipson K, Falk R, Gustafsson J and Camner P 1996 Long-term lung clearance of ^{195}Au-labelled teflon particles in humans *Env. Lung Res.* **22** 65–83

Polig E 2001 Modeling the distribution and dosimetry of internal emitters: a review of mathematical procedures using matrix methods *Health Phys.* **81** 492–501

Press W H, Teukolsky S A, Vetterling W T and Flannery B P 2007 *Numerical Recipes: The Art of Scientific Computing* 3rd edn (Cambridge: Cambridge University Press) chapter 15.5 (Nonlinear Models)

Puncher M and Birchall A 2008 A Monte Carlo method for calculating Bayesian uncertainties in internal dosimetry *Radiat. Prot. Dosim.* **132** 1–12

Takahashi S, Kubota Y, Sato H and Matsuoka O 1993 Retention of ^{133}Ba in the trachea of rabbits, dogs, and monkeys following local administration as $^{133}BaSO_4$ particles *Inhalation Toxicol.* **5** 265–73

Tobin J 1958 Estimation for relationships with limited dependent variables *Econometrica* **26** 24–36

Tran C L and Buchanan D 2000 Development of a biomathematical lung model to describe the exposure–dose relationship for inhaled dust among UK coal miners *IOM Research Report TM/00/02* (Edinburgh: Institute of Occupational Medicine)